Thermally-Prepared Polymorphic Forms of Cilostazol

GRAYSON W. STOWELL,[1] ROBERT J. BEHME,[2] STACY M. DENTON,[2] INIGO PFEIFFER,[1] FREDERICK D. SANCILIO,[1] LINDA B. WHITTALL,[1] ROBERT R. WHITTLE[1]

[1]aaiResearch, Inc., 2320 Scientific Park Drive, Wilmington, North Carolina 28405

[2]Science Resources, Inc., 2029 Washington Avenue, Suite 201, Evansville, Indiana 47714

Received 8 March 2002; revised 8 May 2002; accepted 5 July 2002

ABSTRACT: Prior to this study, cilostazol, an antithrombotic drug, was thought to exist as a single crystalline phase with a melting point of ~159°C (Form A). On cooling, melts often form a glass that, when heated, may crystallize as additional crystalline polymorphic forms. Cilostazol, when reheated, subsequently forms polymorphs that melt at ~136°C (Form B) and 146°C (Form C). Free-energy temperature diagrams estimated from calorimetry data reveal that each pair of the cilostazol polymorphs (A–B, B–C, and A–C) is monotropic. Essentially pure samples of suitable crystalline shape and size permitted single crystal structural analysis of Forms A and C. Theoretical solubility ratios calculated using calorimetry data indicate that at 37°C, Form B should be more than four times more soluble and Form C should be more than two times more soluble than Form A. Forms B and C could not be crystallized from solvents. Metastable forms from super cooled melts analyzed by intrinsic dissolution and Fourier transform-Raman experiments demonstrated that Forms B and C undergo a rapid, solvent-mediated recrystallization to Form A, making dissolution rate measurements difficult. © 2002 Wiley-Liss, Inc. and the American Pharmaceutical Association J Pharm Sci 91:2481–2488, 2002
Keywords: pharmaceutical; thermal analysis; diffraction; heat of fusion; entropy

INTRODUCTION

It is well recognized that polymorphs can significantly impact the overall characteristics of pharmaceuticals.[1] Accordingly, identification, characterization, and control of the specific polymorphic form of an active pharmaceutical ingredient (API) early in the development process is of significant importance. Consequently, potential problems during development or after the product enters the marketplace are minimized or, ideally, eliminated. Furthermore, investigation of polymorphic activity may also give rise to different crystalline forms with altered characteristics compared with those of forms currently under development. This investigation into polymorphs may lead to new, additional, or even second-generation products with enhanced or different therapeutic activity.

Often, potential compounds for drug use have undesirable characteristics, such as poor stability, solubility, and/or bioavailability. Finding an alternate, yet stable polymorphic form with better pharmaceutically desirable characteristics is a substantial benefit to the long-term viability of the drug. In the case of cilostazol, an antithrombotic agent, the only crystalline form reported has renowned poor solubility in acidic, basic, and aqueous media.[2] To improve the solubility of cilostazol and potentially improve its bioavailability, an investigation into potential polymorphic forms of the drug was initiated. Various techniques, including chemical, mechanical, and thermal manipulation were used to induce various polymorphic forms of the drug. During these studies, an amorphous form and two additional

Correspondence to: Robert R. Whittle (Telephone: 910-254-7193; Fax: 910-254-4535;
E-mail: bob.whittle@aai-research.com)

Journal of Pharmaceutical Sciences, Vol. 91, 2481–2488 (2002)

crystalline polymorphic forms were discovered. Characterization of the additional polymorphs involved a multitude of classical and solid-state analytical techniques, including thermal analysis, hot-stage microscopy, X-ray diffraction, spectroscopic methods, intrinsic dissolution, and high-performance liquid chromatography (HPLC).

EXPERIMENTAL SECTION

Materials

Cilostazol, 6-[4-(1-cyclohexyl-1*H*-tetrazol-5-yl)-butoxy]-3,4-dihydro-2(1*H*)-quinolinone (MW = 369.47 amu; Figure 1), was purchased from Laboratorios Phoenix, Buenos Aires, Argentina.

Differential Scanning Calorimetry (DSC)

Initial discovery of cilostazol polymorphism and investigation of temperature programs to prepare individual forms was accomplished with a Mettler-Toledo DSC821^e differential scanning calorimeter. Data acquisition and manipulation was performed with the Mettler-Toledo STAR^e software using ~5–10 mg of sample heated at 10°C/min under nitrogen in sealed vented aluminum pans. Heats of fusion and onset melting points for free-energy difference plots and calculation of theoretical solubility values was accomplished with a Perkin-Elmer DSC4 with TA · PC thermal analysis software. Accurately weighed milligram amounts of material were heated at 20°C/min under nitrogen in sealed vented aluminum pans. Both DSC systems utilize an indium metal reference standard analyzed on each analysis date at the same heating rate to confirm accurate temperature and heat-flow calibration constants.

Hot-stage and Optical Microscopy

Hot-stage microscopy was performed using a Mettler-Toledo FP82HT Hot-stage with an FP90 Central Processor on a Meiji EMZ-TR microscope. Samples were analyzed using a glass slide to visually monitor the formation of the different phases of cilostazol.

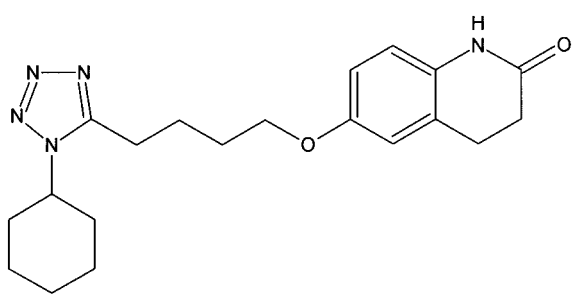

Figure 1. Drawing of cilostazol molecule.

Powder X-ray Diffraction

The powder X-ray diffraction patterns were obtained using a Siemens D500 X-ray Diffractometer with Cu Kα radiation operating at 30 mA and 50 kV. Samples were analyzed on a quartz zero-background sample plate and scanned from 2 to 40° in 2θ, with data points taken every 0.05°at a scan rate of 2.4°/min.

Fourier Transform Infrared (FTIR) and FT-Raman Spectroscopy

FTIR spectra were obtained with a Nicolet Nexus 670 Inspect IR microscope with a micro-ATR attachment. FT-Raman spectra were obtained with a Nicolet Nexus 670 with an FT-Raman attachment, with samples placed in a diffuse reflectance sample holder. The Nicolet OMNIC software package was used for data acquisition and analysis of both types of spectroscopic data.

High-Performance Liquid Chromatography (HPLC)

HPLC analysis of cilostazol was performed to verify the absence of degradation products and integrity of the active pharmaceutical ingredient after the thermal transformation to the different polymorphic forms. The analyses were performed with a Hewlett Packard HP1100 chromatographic system with a variable wavelength diode-array ultraviolet (UV) detector and an Inertsil ODS-3 C18 reversed-phase column (15 cm × 4.6 mm i.d., 3 μm, Metachem Technologies, Torrance, CA). The mobile phase consisted of a mixture of 50 mM potassium phosphate monobasic (pH 6.8) and acetonitrile (55:45 v/v) at a flow rate of 1.0 mL/min. Identification of cilostazol was achieved at a detection wavelength of 254 nm by comparison to the original cilostazol API using the Waters Millenium[32] data acquisition software.

Intrinsic Dissolution

Solubility rate of the different polymorphs was studied by a USP intrinsic dissolution analysis. The dissolution studies were performed with a Van-Kel Vanderkamp 600 Six Spindle Dissolution tester equipped with Van-Kel USP intrinsic dissolution apparatus[3] and a VK650 heater/circulator set at 37°C. Cilostazol pellets were

prepared with a laboratory press and intrinsic dissolution dies. Different sample weights and pressures were tested to optimize pellet formation and subsequently, the dissolution rate. A compression of ~100 mg of cilostazol at 4000 psi for 1 min produced optimal results. FT-Raman analysis was utilized to demonstrate that no polymorphic transition occurred under the high compression used during the formation of the pellets. Different dissolution media and die rotation speeds were evaluated to determine the most appropriate dissolution conditions. Initial intrinsic dissolution studies were carried out using 500 mL of 1% sodium lauryl sulfate (SLS) as the medium, a die rotation speed of 200 rpm, and a pull volume of 5 mL every 30 min up to 6 h, with one additional pull at 24 h. An HP8452A diode array UV-visible spectrophotometer was used to determine the dissolution of the samples against a reference solution at a wavelength of 258 nm. Because of the poor solubility of the drug in aqueous media, more aggressive dissolution conditions were also tested. Ultimately, acetonitrile was also tested as the medium with a die rotation speed of 50 rpm, and a pull volume of 5 mL every 2 min for up to 20 min.

Single-Crystal X-ray Crystallography

Single-crystal X-ray crystallography was performed on a Nonius Kappa-CCD at 294 K with Mo Kα radiation operating at 32 mA and 55 kV. The data were analyzed and the structures determined and refined using the MolEN software system.[4]

Scale-Up Thermal Procedures

Attempts to increase the scale of production of new polymorphic forms were performed using a nitrogen purged programmable oven. The samples were placed in 32-mm aluminum pans and centered in the oven. Multiple heating programs with varying heat rates, hold temperatures, and hold times were initiated to produce the polymorphic forms.

RESULTS AND DISCUSSION

The DSC thermogram of cilostazol API (Form A) heated at 10°C/min, shown in Figure 2a, exhibits only a single endotherm with a melting point of ~159°C, corresponding with previously reported literature values.[2] During heat cycling studies,

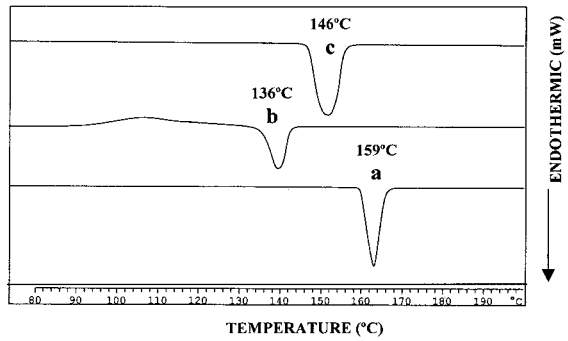

Figure 2. DSC thermograms of cilostazol Form A (a), Form B (b), and Form C (c). Form B and Form C polymorphs formed by heat cycling techniques.

however, cold crystallization occurred and a new melting point at ~136°C was observed (Figure 2b), which is significantly lower than that for Form A.[5] Hot-stage microscopy was used to confirm the presence of this new form and further investigate the thermal behavior of cilostazol. After a sample of cilostazol melted, the cooled sample maintained an amorphous, glassy state. On reheating, a cold crystallization was observed that produced a different crystalline phase, which was confirmed by X-ray powder diffraction (Figure 3) and melted at ~136°C when analyzed by DSC.

The relative stability of Form B was investigated using hot-stage microscopy. Samples from various hold times and temperatures were analyzed by X-ray powder diffraction, which evaluated the relative presence of the crystalline and amorphous forms of cilostazol. During this study, as the heating rate, hold temperature, and hold time increased, the proportion of Form A also increased. During hot-stage microscopy, any outside physical stress applied to the sample after melt (such as probing) induced the spontaneous nucleation of the sample to Form A during the cold crystallization.

To study the thermal preparation of Form B for additional testing, an experimental matrix was designed in which samples of Form A were melted in DSC pans and cooled to specific temperatures ranging from 80 to 130°C and held at that temperature for periods of time of up to 30 min. When analyzed by DSC, these crystallized materials exhibited a variety of melting transitions for Forms A and B, with some samples also exhibiting another melting transition of a third polymorph (Form C) that melted between Forms A and B at ~146°C.[5] Some of the materials crystallized from the melts of Form A resulted in

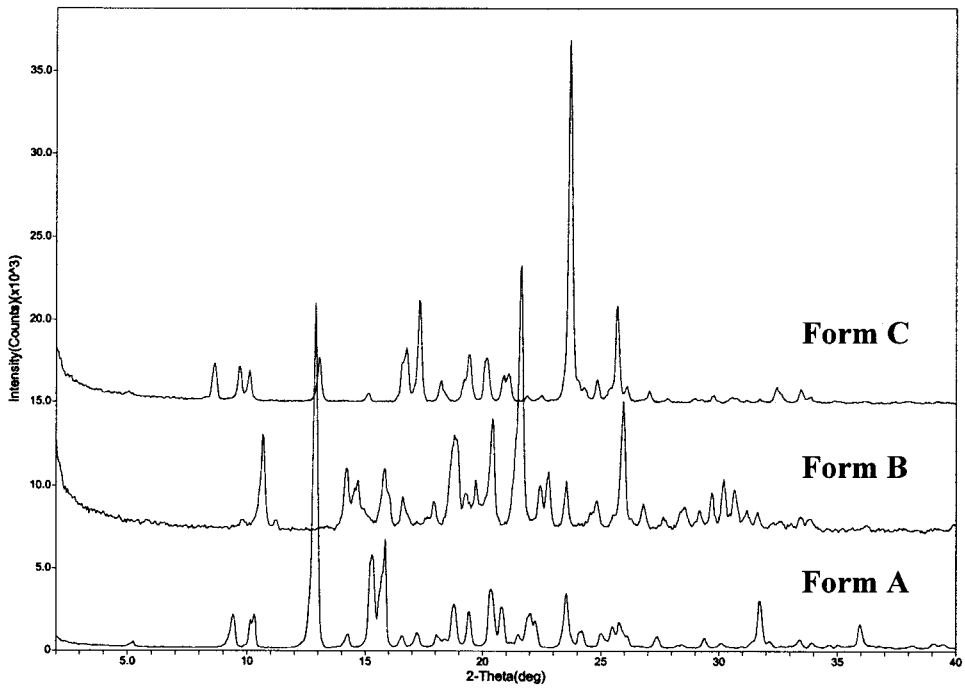

Figure 3. X-ray powder diffraction patterns of cilostazol Form A, Form B, and Form C.

thermal curves with single melting endotherms for Forms A, B, and C (Figure 2), depending on the specific cooling temperature and hold times used.

Based on the experimental results, attempts were made to grow and isolate single crystals suitable for X-ray analysis of each form. Form A crystals were suitable needles and used "as is". Form B existed only as tiny needles crystallized in microcrystalline clusters; therefore, single-crystal structural analysis could not be performed. Suitable plate-like crystals of Form C were isolated from heat cycling with DSC. For example, cilostazol Form A was melted (at >170°C), then cooled to ~0°C and reheated to ~100°C and held for 5 min. This sample was then cooled to ~0°C and reheated to ~145°C and held for 5 min. This procedure causes the Form B crystals to melt, leaving the Form C crystals to act as seeds for further crystallization. The sample was then cooled to ambient temperature to create the plate-like crystals of Form C. A comparison of the crystal structures and unit cells appears in Table 1 for the Form A and Form C crystals. The orientation differences in the two conformational polymorphs are shown in Figure 4. The polymorphs exhibit a major twist of ~108°around the C12-C13-C14-C15 torsional angle, creating distinct differences in the unit cell packing. The full details of these structures will be presented in a concurrent structural publication.[6] Rietveld analysis using microcrystalline Form B material may yield structural parameters and data on its crystalline state.

A wide variety of heat-cycled DSC studies confirm that initiation and completion of crystallization of the various polymorphic forms of cilostazol are time and temperature dependent. Typically, Form B crystallizes first. With continued heating, Form B converts to Form A. Crystallization from the melt is an exothermic process,

Table 1. Single-Crystal X-Ray Parameters for Form A and Form C

Parameter Class Space Group	Form A Orthorhombic *P*bca	Form C Monoclinic $P2_1/n$
a (Å)	11.324 (1)	5.148 (1)
b (Å)	9.855 (1)	10.739 (1)
c (Å)	35.012 (1)	35.279 (1)
β (°)	—	94.070 (1)
Z	8	4
V (Å^3)	3907.3 (5)	1945.3 (6)
ρ_{calc} (g/cm^3)	1.256	1.262
R, R_w	0.042, 0.042	0.043, 0.041

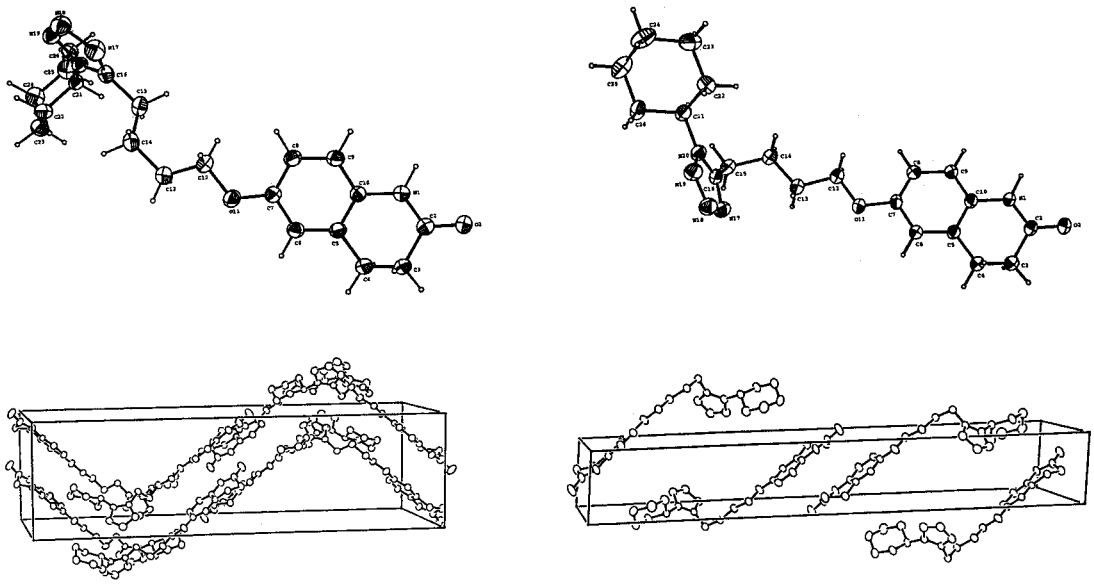

Figure 4. ORTEP representation of Form A (top left) and Form C (top right) and view of unit cells perpendicular to the c-axis (Form A, bottom left; Form C, bottom right).

and monitoring the process with DSC determined when crystallization started and also when crystallization was complete. Some crystallized solids from cilostazol melts were polymorphically pure Form B, which melts at ~136°C, with an apparent heat of fusion of 105.2 ± 3.9 J/g. Form A melts at ~159°C, with a heat of fusion of 127.7 ± 1.4 J/g. According to the heat of fusion rule,[7] Forms A and B are monotropic, which means that crystalline Form A is physically more stable than Form B at all temperatures below its melting point. Conversely, Form B may spontaneously change to Form A, but not vice versa. Form C proved the most difficult to obtain for testing. On several occasions, polymorphically pure Form C was crystallized and analyzed by DSC to show a melt at ~146°C, with a heat of fusion of ~115.7 ± 0.3 J/g. Because the heat of fusion of Form C is intermediate between those of Forms A and B, the heat of fusion rule suggests that each pair of cilostazol polymorphs (A–B, A–C, and B–C) is monotropic.

Using an approach described by Yu and coworkers,[8,9] and assuming that the difference in heat capacity for each polymorphic pair is about zero, free energy difference plots versus temperature for cilostazol polymorphs were calculated using eq. 1:

$$\Delta G_{(\mathrm{A}\rightarrow\mathrm{A,\ B\ or\ C})} = \Delta H_{(\mathrm{A}\rightarrow\mathrm{A,\ B,\ or\ C})} - T\Delta S_{(\mathrm{A}\rightarrow\mathrm{A,\ B\ or\ C})} \quad (1)$$

The heats of fusion and entropy values estimated from calorimetry data that are summarized in Table 2.

Plots of the resulting free energy curves versus temperature (i.e., the free energy differences between Forms A to A, Forms A to B, and Forms A to C) according to eq. 1 are shown in Figure 5.

Table 2. Calorimetry Data for Free-Energy Temperature Diagrams, Theoretical Solubility Ratios, and Virtual Transition Temperatures[a]

Parameter	Form A	Form B	Form C
T_m, °C	159.0 ± 0.5	135.8 ± 0.2	146.0 ± 0.5
T_m, K	432.0 ± 0.5	408.8 ± 0.2	419.0 ± 0.5
ΔH_f, J/g	127.7 ± 1.4	105.2 ± 3.9	115.7 ± 0.3
ΔH_f, kJ/mol	4.717 ± 0.53	3.888 ± 1.45	4.275 ± 0.11
ΔS, J mol^{-1} K^{-1}[b]	109.2	95.1	102.0

[a] Virtual transition temperatures, T_{vt}: forms B and C, 288°C; forms B and A, 315°C; forms C and A, 341°C.
[b] $\Delta S = \Delta H_f / T_{m,\ K}$.

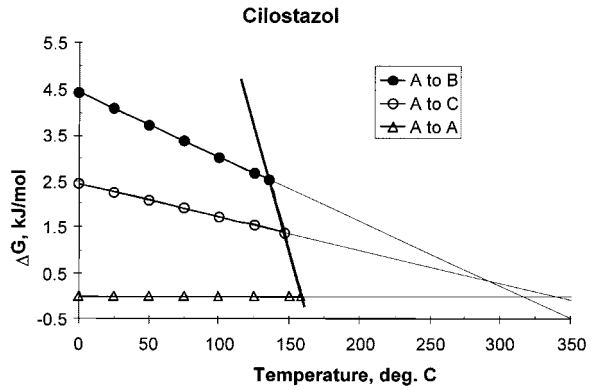

Figure 5. Free energy difference plots versus temperature for three anhydrous polymorphs of cilostazol.

In Figure 5, the solid bold line represents liquefied (melted) cilostazol. The free energy curve of liquefied cilostazol intersects the free energy difference plots at the melting point of each polymorph. At temperatures below the melting points, the liquid free energy curve is that of the supercooled melt. The free energy difference plots for the cilostazol polymorphic pairs indicate that Form B has the largest free energy difference to Form A at all temperatures below its melting point. Form A has the lowest free energy, and the free energy of Form C is intermediate between those of Forms B and A. The free energy difference plots of the polymorphs do not intersect below the melting points. Each pair of polymorphs is monotropic, and Form A is thermodynamically the most physically stable polymorph. The free energy difference plots apparently intersect at virtual transition temperatures (T_{vt}), well above their melting points. At a virtual transition temperature, two polymorphs have the same free energy. Because the difference in their free energies is zero, the virtual transition temperature is the difference between their heats of fusion divided by the difference in their entropies. Calculated virtual transition temperatures appear in Table 2.

Metastable forms often crystallize from solution, but when left in the solvent, metastable forms dissolve and crystallize as the least soluble, most stable form. Although metastable forms of cilostazol could not be crystallized by conventional seeding or rapid solvent evaporation, other more aggressive approaches, such as from supercritical fluids, might prove successful.[10] Metastable Form B, however, was readily obtained without solvents by crystallization from amorphous supercooled melts, perhaps because Form B has the lowest degree of order; that is, it has the smallest difference in entropy between it and the amorphous liquid (Table 2).

Grant and Higuchi and Grant and Gu have described in detail mathematical models to estimate polymorph solubility.[11,121] Equations 2 and 3 for each of two polymorphs when combined result in eq. 4, which is an expression for the ratio of their activities in solution.

$$G_I - G_0 = \Delta G_I^0 = \Delta H_I^0 - T\Delta S_I^0 = RT \ln\left(\frac{a_I}{1}\right) \quad (2)$$

$$G_{II} - G_0 = \Delta G_{II}^0 = \Delta H_{II}^0 - T\Delta S_{II}^0 = RT \ln\left(\frac{a_{II}}{1}\right) \quad (3)$$

$$\Delta G_{I\rightarrow II} = \Delta H_{I\rightarrow II}^0 - T\Delta S_{I\rightarrow II}^0 = RT \ln\left(\frac{a_{II}}{a_I}\right) \quad (4)$$

The ratio of the activities is proportional to ratios of their fugacity, vapor pressure, molality, and solubility as long as Henry's law is obeyed. Equation 4 was rearranged to eq. 5 and was used to calculate solubility ratios versus temperature where free energy differences were calculated using calorimetry data with eq. 1 for each polymorphic pair.

$$\frac{a_{II}}{a_I} = \frac{m_{II}}{m_I} = e^{\left(\frac{\Delta G_{I\rightarrow II}}{RT}\right)} \quad (5)$$

The calculated free energy differences from which solubility ratios were calculated at a variety of temperatures for three pairs of cilostazol polymorphs are listed in Table 3. Calorimetry data suggest that at 37°C, Form B should be at least four times more soluble than Form A, Form C two times more soluble than Form A, and Form B about two times more soluble than Form C in any ideal solvent.

Crystallization of cilostazol from various solvents or with seed crystals of Form B or Form C and rapid quenching to produce Form B or Form C proved unsuccessful and resulted in the formation of only Form A. A nitrogen-purged programmable oven that was set up to simulate the DSC conditions proved successful in making the new polymorphs on a larger scale. However, layering of the different polymorphs was observed when preparing the samples on a larger scale, indicating insufficient heat distribution and transfer under the conditions used. For example, Form B could be formed in appreciable amounts, but Form C was always present as a crust on the top of the sample cake (Figure 6). This phenomenon was

Table 3. Calculated Free Energies and Solubility Ratios for Cilostazol Polymorphs

Temperature		$\Delta G = \Delta H - T\Delta S$ (J/mol)			$e^{\left(\frac{\Delta G}{RT}\right)}$		
°C	K	A to B	A to C	C to B	m_B/m_A	m_C/m_A	m_B/m_C
0	273	4441	2454	1986	7.1	2.9	2.4
25	298	4088	2274	1814	5.2	2.5	2.1
37	310	3919	2188	1731	4.6	2.3	2.0
50	323	3736	2094	1641	4.0	2.2	1.8
75	348	3383	1914	1469	3.2	1.9	1.7
100	373	3031	1734	1296	2.7	1.7	1.5
125	398	2678	1554	1124	2.2	1.6	1.4
150	423	2326	1374	951.3	1.9	1.5	1.3

also observed when attempting to make pure Form C, with Form A present as a crust on the top of the cake. The material isolated and subsequently used for dissolution studies contained approximately equal mixtures of Form B and Form C.

Intrinsic dissolution studies performed using 1% SLS as the medium indicated that the intrinsic dissolution rate (IDR) of Form A (sample 1) and the mixture of Forms B and C (sample 2) of cilostazol were similar. These results were unexpected because theoretical calculations indicated that Forms B and C, with lower melting points, were expected to dissolve faster than Form A. FT-Raman analysis of the cilostazol pellets indicated that a portion of cilostazol sample 2 converted to crystalline Form A on the pellet surface exposed to dissolution media, but pellets not exposed to dissolution media had not converted. In an attempt to increase the dissolution rate beyond the solvent-mediated transformation rate, acetonitrile was selected as the media. The results showed that the IDR of sample 2 exceeded that of sample 1. However, FT-Raman demonstrated that some conversion to the more stable polymorphic form had still taken place under these conditions (Figure 7). To effectively utilize Forms B and C of cilostazol in pharmaceutical products, care must be taken to develop a formulation that protects against or minimizes the conversion to Form A.

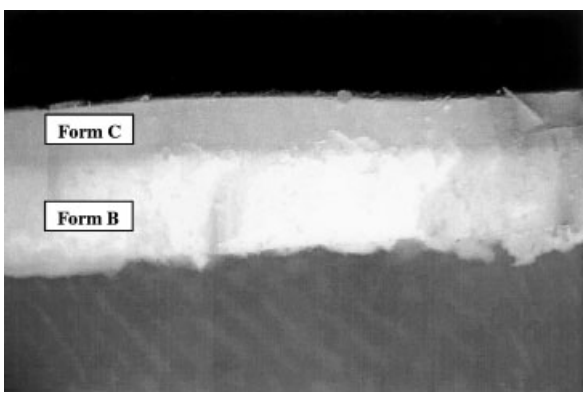

Figure 6. Magnified cross-section (40×) of cilostazol cake after processing in a programmable oven.

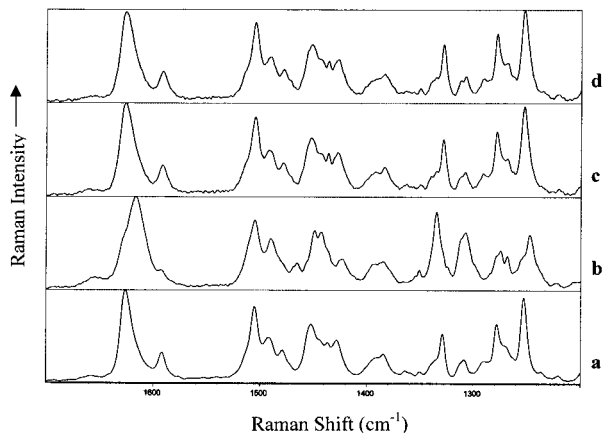

Figure 7. FT-Raman spectra of sample 1 (Form A) (a), initial sample 2 (Forms B and C) (b), sample 1 after intrinsic dissolution in acetonitrile (c), and sample 2 after intrinsic dissolution in acetonitrile (d).

REFERENCES

1. 1999. For a general reference for polymorphs in the drug industry see Byrn SR, Pfeiffer RR, Stowell JG. Solid-state chemistry of drugs, 2nd ed. West Lafayette, IN: SSCI.
2. Shimizu T, Osumi T, Niimi K, Nakagawa K. 1985. Physico-chemical properties and stability of cilostazol. Arzneim-Forsch/Drug Res 35:1117–1123.

3. United States Pharmacopoeial Convention, Inc. 2001. The pharmacopoeia of the United States, 25th Revision. Rockville, MD: pp. 2159–2160.
4. OpenMolen: Interactive intelligent structure solution. 1997. Delft. The Netherlands: Nonius B.V.
5. Stowell GW, Whittle RR. U.S. Patent 6,388,080 (May 14, 2002) and other Patents Pending.
6. Whittall LB, Whittle RR, Stowell GW. 2002. Polymorphic forms of cilostazol. Acta Cryst C58:525–527.
7. Burger A, Ramberger R. 1979. On the polymorphism of pharmaceuticals and other molecular crystals. I Theory of thermodynamic rules. II Applicability of thermodynamic rules. Mikrochim Acta [Wien] 2:259–271.
8. Yu L. 1995. Inferring thermodynamic stability relationship of polymorphs from melting data. J Pharm Sci 84:966–974.
9. Yu L, Stephenson GA, Mitchell CA, Bunnell CA, Snorek SV, Bowyer JJ, Borchardt TB, Stowell JG, Byrn SR. 2000. Thermochemistry and conformational polymorphism of a hexamorphic crystal system. J Am Chem Soc 122:585–591.
10. Beach S, Latham D, Sidgewick C, Hanna M, York P. 1999. Control of the Physical Form of Salmeritol Xinafoate. Organic Process Res Devel 3:370–376.
11. Grant DJW, Higuchi T. 1990. Solubility behavior of organic compounds. New York: John Wiley & Sons. pp. 12–38.
12. Gu CH, Grant DJW. 2001. Estimating the relative stability of polymorphs and hydrates from heats of solution and solubility data. J Pharm Sci 90:1277–1287.